

## Supporting Information

# Copper Molybdenum Sulfide: A New Efficient Electrocatalyst for Hydrogen Production from Water

**Phong D. Tran,\*<sup>a</sup> Mai Nguyen,<sup>a</sup> Stevin S. Pramana,<sup>b,c</sup> Anirban Bhattacharjee,<sup>d</sup> Sing Yang Chiam,<sup>e</sup> Jennifer Fize,<sup>f</sup> Martin J. Field,<sup>d</sup> Vincent Artero,\*<sup>f</sup> Lydia H. Wong,<sup>b</sup> Joachim Loo,<sup>b</sup> James Barber\*<sup>b,g</sup>**

<sup>a</sup>*Energy Research Institute @ NTU, Nanyang Technological University, Singapore; Email: [dptran@ntu.edu.sg](mailto:dptran@ntu.edu.sg)*

<sup>b</sup>*Solar Fuel Laboratory, School of Materials Science and Engineering, Nanyang Technological University, Singapore. Email: [j.barber@imperial.ac.uk](mailto:j.barber@imperial.ac.uk)*

<sup>c</sup>*Facility of Analysis, Characterization, Testing and Simulation (FACTS), Nanyang Technological University, Singapore*

<sup>d</sup>*DYNAMO Team/DYNAMOP Group, Institut de Biologie Structurale “Jean-Pierre Ebel” (UMR9075 CEA/CNRS/Université Grenoble 1), Grenoble, France*

<sup>e</sup>*Institute of Materials Research and Engineering, ASTAR, Singapore*

<sup>f</sup>*Laboratoire de Chimie et Biologie des Métaux, Université Grenoble 1/CNRS/CEA, Grenoble, France; Email : [vincent.artero@cea.fr](mailto:vincent.artero@cea.fr)*

<sup>g</sup>*Division of Molecular Biosciences, Imperial College London, London SW7 2AZ, UK*

## 1. General

$\text{Cu}_2\text{O}$ ,  $(\text{NH}_4)_2[\text{MoS}_4]$ ,  $\text{HBF}_4 \cdot \text{Et}_2\text{O}$  were purchased from Sigma Aldrich. Analytical grade acetonitrile (MeCN) and dimethyl formamide (DMF) were purchased from Sinopharm Chemical. All chemical compounds were used as received without any purification.  $[\text{Cu}(\text{MeCN})](\text{BF}_4)$  was prepared from  $\text{Cu}_2\text{O}$  and  $\text{HBF}_4 \cdot \text{Et}_2\text{O}$  in degassed MeCN solution following reported process [1].  $[\text{Cu}(\text{MeCN})](\text{BF}_4)$  colorless powder was carefully dried under vacuum at room temperature.

## 2. Synthesis of $\text{Cu}_2\text{MoS}_4$

In 40mL degassed DMF/MeCN (v/v = 1/1) solvent was added 300mg  $[\text{Cu}(\text{MeCN})](\text{BF}_4)$  (1.56mmol) and 203 mg  $(\text{NH}_4)_2[\text{MoS}_4]$  (0.78mmol). Reaction solution was refluxed for 1 day at 135°C under  $\text{N}_2$  atmosphere. Subsequently, dark-red crystalline product was isolated from the reaction mixture, carefully washed with deionised water, ethanol and dried overnight in a vacuum oven.

## 3. Structural and chemical composition characterizations

Powder X-ray diffraction pattern of  $\text{Cu}_2\text{MoS}_4$  was collected at room temperature from 10 to 80°  $2\theta$  with a step size of 0.02° using Bruker D8 Advance (XRD, Cu-K $\alpha$  radiation) equipped with 1D Lynxeye detector. The crystal structure of  $\text{Cu}_2\text{MoS}_4$  was refined by Rietveld analysis<sup>XX</sup> using a fundamental parameter peak shape profile<sup>YY</sup> implemented in Topas Version 3<sup>ZZ</sup>. A seven-coefficient Chebychev polynominal, a zero error, unit cell parameters, scale factor, crystal size and spherical harmonics preferred orientation were refined sequentially. The atomic positions were fixed according to the  $\text{Cu}_2\text{WS}_4$  reference [2]. The unit cell and atomic parameters are shown in **Table S1**.

To address the charging issue,  $\text{Cu}_2\text{MoS}_4$  powder was drop-casted onto fluorine-doped tin oxide (FTO) substrate.  $\text{Cu}_2\text{MoS}_4/\text{FTO}$  samples were transferred *ex-situ* to a VG

ESCALAB 220i-XL X-ray photoelectron spectroscopy (XPS) system equipped with a hemispherical analyzer. The background pressure in the analysis chamber was in the  $10^{-10}$  Torr range. The analyzer was calibrated with gold, silver, and copper polycrystalline standard samples by setting the Au  $4f_{7/2}$ , Ag  $3d_{5/2}$  and Cu  $2p_{3/2}$  peaks at binding energies of  $83.98 \pm 0.02$ ,  $368.26 \pm 0.02$ , and  $932.67 \pm 0.02$  eV. In order to minimize charging, a Mg  $\text{k}\alpha$  x-ray source at a low power of 180W together with low energy electron flood gun was used. The survey and high-energy resolution scans were recorded with pass energies of 150 and 20 eV, respectively. The XPS spectra were examined by curve fitting using a combination of Gaussian and Lorentzian line shapes.

#### **4. Electrocatalytic activities assays**

##### **4.1 Cu<sub>2</sub>MoS<sub>4</sub> electrode fabrication**

3mg Cu<sub>2</sub>MoS<sub>4</sub> was suspended in stock solution containing 0.8mL deionized H<sub>2</sub>O, 0.2mL ethanol and 10  $\mu$ L nafion®117 solution (5%) by ultra-sonication for 30 min. 1  $\mu$ L of this homogeneous stable suspension was drop-casted on carbon glassy electrode surface (d = 3mm). After air-drying, the Cu<sub>2</sub>MoS<sub>4</sub>/carbon electrode was further dried in vacuum at room temperature for hours before use.

For bulk electrolysis experiments, Cu<sub>2</sub>MoS<sub>4</sub> catalyst was loaded onto FTO electrode. Typically, 14 $\mu$ L of Cu<sub>2</sub>MoS<sub>4</sub> solution was diluted with 0.5mL water/ethanol solution (v/v = 4/1). This 0.5 mL diluted solution was then drop-casted onto 1.0cm<sup>2</sup> FTO electrode surface, air-dried and subsequently dried in a vacuum oven for hours before use. By doing so, we obtained a Cu<sub>2</sub>MoS<sub>4</sub>/FTO electrode with a similar mass catalyst loading to that of the Cu<sub>2</sub>MoS<sub>4</sub>/carbon electrode (ca. 0.0416 mg ( $1.181 \cdot 10^{-7}$  mol) Cu<sub>2</sub>MoS<sub>4</sub>/ cm<sup>2</sup> electrode).

## 4.2 Electrochemical analysis

Electrochemical analysis was done using a CHI, model 852 or a BioLogic science instrument SP300 potentiostat. Three electrodes configuration was employed. The working electrode was Cu<sub>2</sub>MoS<sub>4</sub>/carbon or Cu<sub>2</sub>MoS<sub>4</sub>/FTO electrode, the reference electrode was Ag/AgCl, 3M KCl and the counter electrode was a Pt mesh. pH0 H<sub>2</sub>SO<sub>4</sub> (0.5M) or pH6, pH7 phosphate buffer (0.1M) solution was used as electrolyte. Electrolyte solution was carefully saturated with research grade hydrogen before use to eliminate dissolved oxygen. Hydrogen bubbling was kept continuously during measurements. Potentials measured versus the Ag/AgCl electrode were converted to versus RHE by using the following formula:

$$E_{\text{vs RHE}} = E_{\text{vs Ag/AgCl}} + 0.059 \cdot \text{pH} + 0.210 \text{ (V).}$$

Bulk electrolysis was done in a gas-tight electrochemical cell that was constantly flushed with nitrogen (5mL·min<sup>-1</sup>). To quantify hydrogen produced, the output gas was automatically sampled (100µL) every 2 min and analyzed in a Perkin-Elmer Clarus 500 gas chromatograph equipped with a Waters Porapack Q 80/100 column (6' 1/8") thermostated at 40°C and a thermal conductivity detector (TCD) thermostated at 100°C. The retention time of H<sub>2</sub> was 2.1 min. Calibration was performed via chrono-potentiometric experiments involving a platinum working electrode immersed in a 0.1M sulfuric acid solution, for which the Faradaic yield of H<sub>2</sub> production was considered to be unitary.

## 5. DFT calculations

The crystal structure of the Cu<sub>2</sub>MoS<sub>4</sub> material consists of sheets formed by interlinked copper and molybdenum atoms, tetrahedrally coordinated to bridging sulfur atoms. The sheets have a square planar arrangement and each sulfur coordinates to two Cu atoms and one Mo. This system can, in principle, be modeled using two-dimensional periodic quantum chemical

(QC) methods but in this work we employ a minimal truncated model consisting of one Mo and four Cu atoms with their sulfur coordination spheres. The unsatisfied valencies on the sulfurs, caused by truncating the crystal structure, are filled by the addition of methyl groups. The structure was then geometry optimized, keeping the positions of all atoms fixed, other than the methyl carbon and hydrogens. Optimization of this frozen model was first done with a force field potential and then with a density functional theory (DFT) method. After this methyl group refinement, the complete structure was geometry optimized at the DFT level of theory. In this calculation, all atoms were free to move, except the methyl group carbons, which were fixed at their previously-determined positions. This DFT-optimized model structure served as the starting point for the construction of all the species that we investigated in the catalytic cycle. Given the radical approximations made in generating this calculational model from the experimental structure of the material, we do not expect to obtain quantitative energetic results for the system. Nevertheless, we aim to obtain qualitative insights into how the catalysis at the surface occurs.

All DFT geometry-optimizations were performed with the BP86 functional and the TZVP basis set using the ORCA QC program (version 2.9.1). Solvent effects were included in all calculations using a COSMO implicit solvation model appropriate for water. ECPs were used for Mo and Cu atoms with 28 and 10 core electrons, respectively. The parameters for the Mo and Cu ECPs were obtained from the pseudopotential library of the Stuttgart/Cologne group [3] and the corresponding basis sets from the EMSL Basis Set Library [4,5]. The point charges and spin populations were obtained using natural population analysis, performed using the program GENNBO interfaced to ORCA [6].

## Supplementary Data

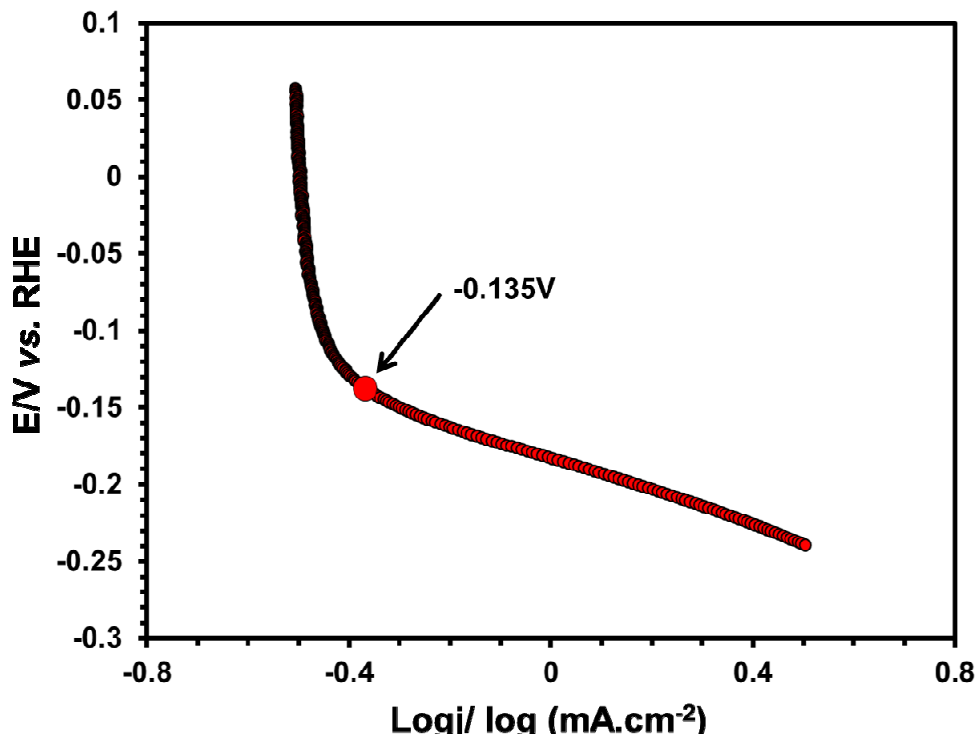


**Figure S1:** The Tafel plot of  $\text{Cu}_2\text{MoS}_4$  catalyst

The onset-potential for HER was read from the Tafel plot (**Figure S1**). For example, the Tafel plot of the  $\text{MoS}_2$  catalyst shows a linear relationship in the region of low current densities and for potentials below -0.135V. But it starts to deviate above -0.133V. Therefore, -0.135V was read as the onset potential for the  $\text{MoS}_2$  catalyst.

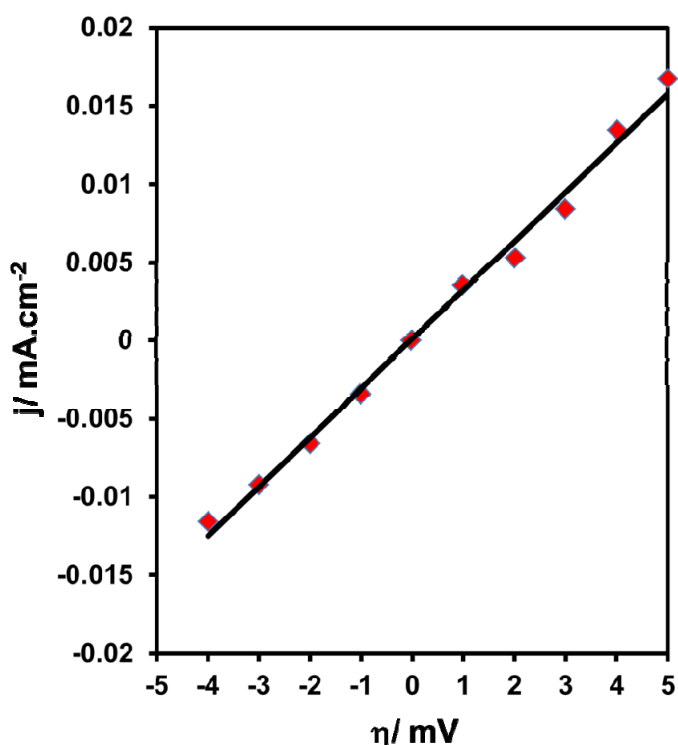


**Figure S2:** Current-potential curve for hydrogen electrode reaction on a  $\text{Cu}_2\text{MoS}_4$  electrode in  $\text{H}_2$ -saturated pH 7 phosphate buffer solution (0.1M) in the linear polarization region of small overpotentials. Potential scan rate:  $2\text{mV.s}^{-1}$

Exchange current density of  $0.040 \text{ mA.cm}^{-2}$  was determined for  $\text{Cu}_2\text{MoS}_4$  catalyst based on the slope in **figure S2** and following the method described by Inoue *et al* [7].

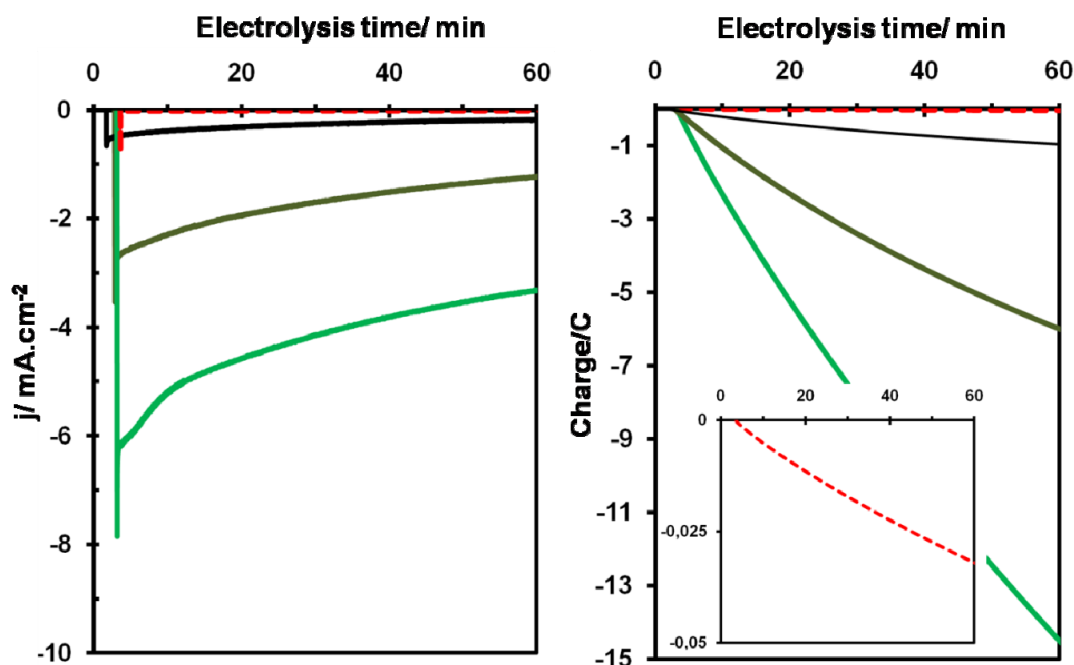


**Figure S3:** **Left:** Catalytic current evolution versus electrolysis time using a  $\text{Cu}_2\text{MoS}_4/\text{FTO}$   $1\text{cm}^2$  electrode in pH 7 phosphate buffer at different potentials (black: -0.2, grey: -0.3, and green: -0.4V vs. RHE). **Right:** Charge (in Coulomb) evolution corresponding to catalytic  $\text{H}_2$  generation versus electrolysis time at different potentials (black: -0.2, grey: -0.3, and green: -0.4V vs. RHE). pH 7 electrolyte solution and using  $\text{Cu}_2\text{MoS}_4/\text{FTO}$  electrode. Current and charge passed through a control FTO  $1\text{cm}^2$  electrode without  $\text{Cu}_2\text{MoS}_4$  catalyst is presented as reference (the red curve).

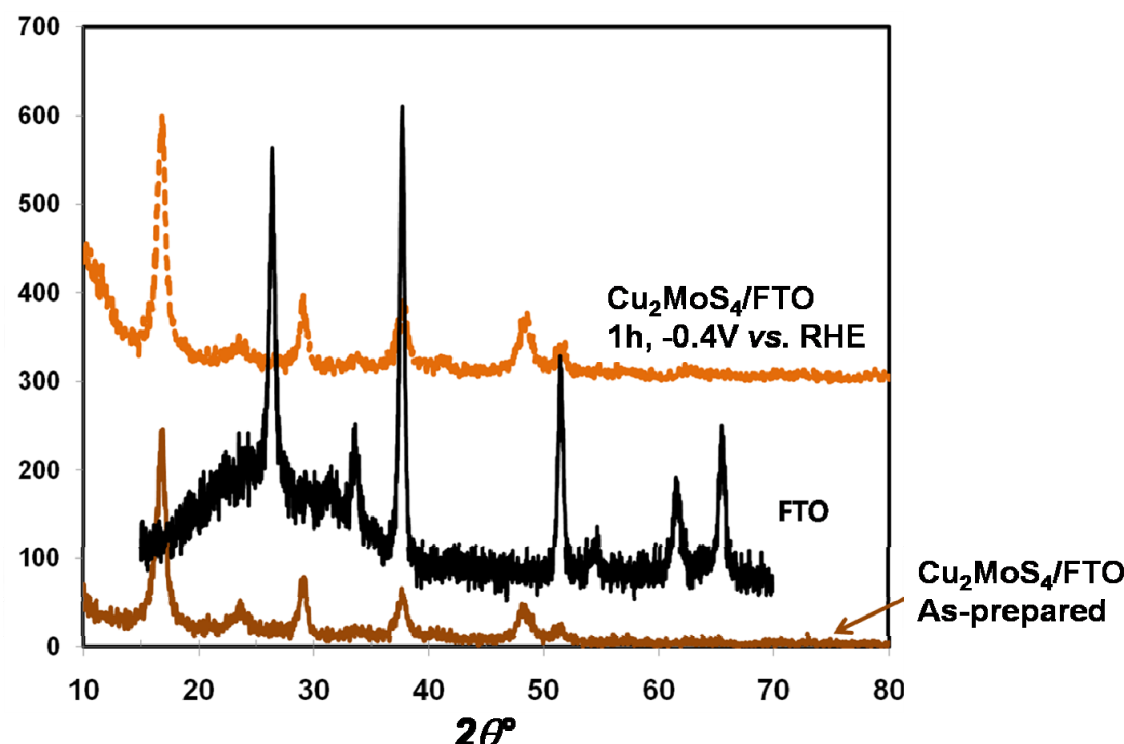


**Figure S4:** XRD analysis on Cu<sub>2</sub>MoS<sub>4</sub>/FTO electrode: as prepared and after being held at -0.4V vs. RHE in a pH 7 electrolyte solution for 1h (hydrogen was generated at this potential)

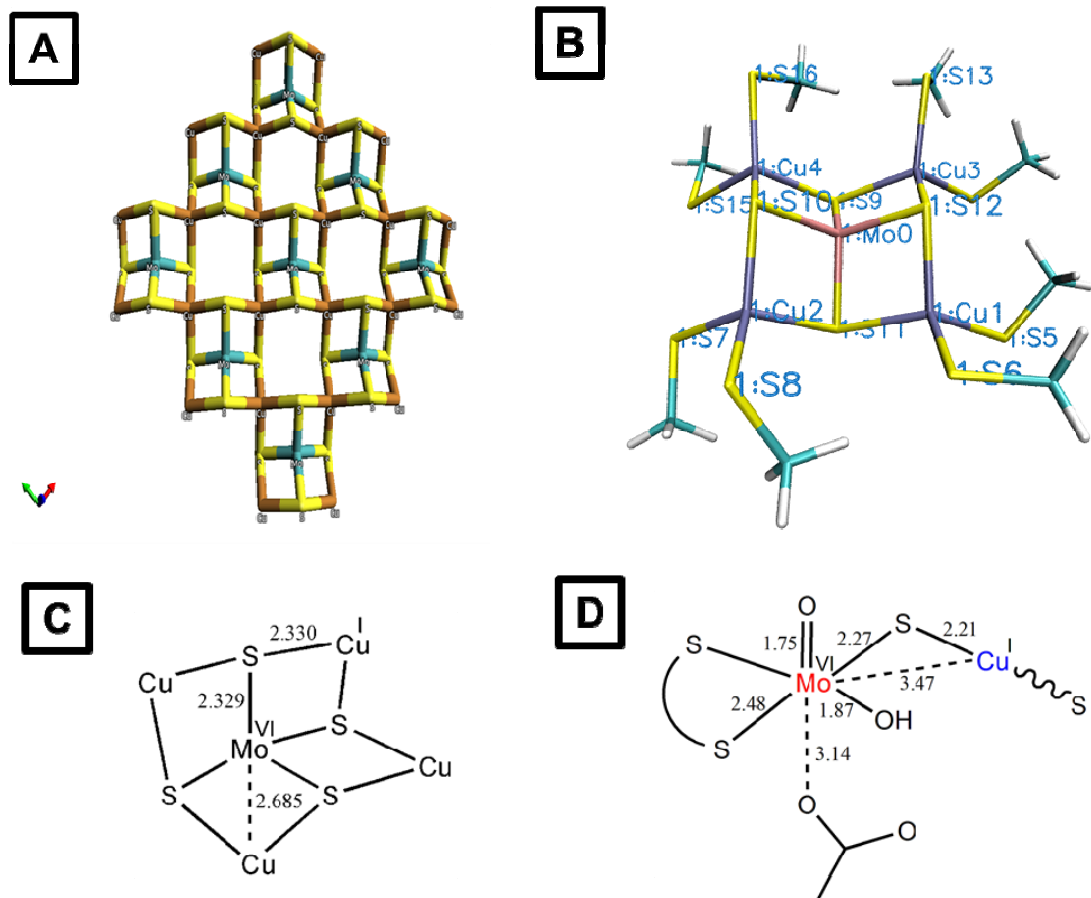


**Figure S5:** Depiction of the crystal structure (A), the DFT-optimized structure of the model compound **M** (B), depicted structures of the  $[MoS_4Cu_4]$  building block (C) and the catalytic active site of molybdenum CO-dehydrogenase (D).

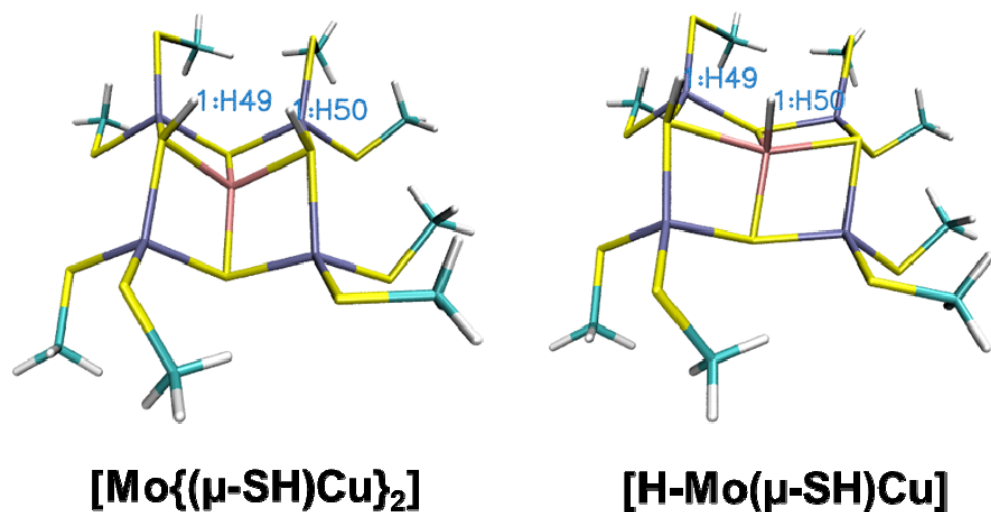


**Figure S6:** DFT-optimized (BP86 functional) structures of the two intermediates identified for  $\text{H}_2$  evolution.

**Table S1.** Comparison of the structural properties of the X-ray crystallographic structure and the DFT-optimized model **M** with the BP86 functional. Distances are in Å and angles in degrees.

Internal Coordinate	Experiment	<b>M</b>
Cu(3)-S(12)	2.340	2.379
Cu(2)-S(11)	2.340	2.398
Cu(2)-S(10)	2.340	2.375
Mo-S(12)	2.329	2.271
Cu(1)-S(12)	2.340	2.397
Cu(3)-S(9)	2.340	2.393
Mo-S(11)	2.329	2.269
Mo-S(10)	2.329	2.291
Mo-Cu(1)	2.685	2.838
Cu(4)-S(10)	2.340	2.371
Cu(1)-S(11)	2.340	2.367
Mo-Cu(3)	2.685	2.835
Mo-Cu(2)	2.685	2.846
Mo-S(9)	2.329	2.262
Cu(4)-S(9)	2.340	2.411
Mo-Cu(4)	2.685	2.845
Cu(1)-S(12)-Cu(3)	108.5	113.1
S(10)-Mo(0)-S(12)	108.1	111.8
Cu(4)-S(10)-Cu(2)	108.5	112.4
S(9)-Mo(0)-S(11)	108.1	111.0

**Table S2.** DFT-optimized (BP86 functional) structures of the two intermediates identified for H<sub>2</sub> evolution (See Figure 5). Distances are in Å and angles in degrees.

Internal Coordinate	[H-Mo(μ-SH)Cu]	[Mo{(\mu-SH)Cu} <sub>2</sub> ]
Cu(3)-S(12)	2.34	2.43
Cu(2)-S(11)	2.38	2.43
Cu(2)-S(10)	2.40	2.40
Mo-S(12)	2.34	2.38
Cu(1)-S(12)	2.35	2.49
Cu(3)-S(9)	2.37	2.40
S(12)-H(50)	-	1.40
Mo-H(50)	2.48	-
Mo-S(11)	2.28	2.26
Mo-S(10)	2.63	2.38
H(49)-H(50)	2.14	2.10
S(10)-H(49)	1.37	1.40
Mo-Cu(1)	2.86	2.89
Cu(4)-S(10)	2.38	2.41
Cu(1)-S(11)	2.35	2.37
Mo-Cu(3)	2.89	2.86
Mo-Cu(2)	3.19	2.88
Mo-S(9)	2.26	2.25
Cu(4)-S(9)	2.39	2.43
Mo-Cu(4)	3.06	2.90
Cu(4)-S(10)-Cu(2)	127.48	116.32
S(10)-Mo(0)-S(12)	141.62	94.30
Cu(3)-S(9)-Cu(4)	133.21	108.31
S(9)-Mo(0)-S(11)	109.63	126.09
Cu(2)-S(11)-Cu(1)	133.53	108.49
Cu(1)-S(12)-Cu(3)	109.29	119.62

**Table S3.** Natural charge and spin population (into brackets) analysis for **M** and the two intermediates identified for H<sub>2</sub> evolution (See Figure 5).

Atom	<b>M</b>	[H-Mo(μ-SH)Cu]	[Mo{( $\mu$ -SH)Cu} <sub>2</sub> ]
Cu(1)	0.74856 (0.0)	0.76349 (0.0)	0.74767 (0.04956)
S(11)	-0.51535 (0.0)	-0.55032 (0.0)	-0.52056 (0.03777)
Mo	-0.15331 (0.0)	-0.14688 (0.0)	-0.14646 (0.49858)
Cu(4)	0.74483 (0.0)	0.72378 (0.0)	0.74477 (0.04499)
S(10)	-0.5948 (-0.0)	-0.57628 (-0.0)	-0.41247 (-0.0105)
H(49)	N/A (N/A)	0.18041 (-0.0)	0.1579 (0.01242)
Cu(3)	0.75833 (0.0)	0.76704 (-0.0)	0.75802 (0.04858)
Cu(2)	0.74468 (0.0)	0.71643 (-0.0)	0.74542 (0.04611)
S(12)	-0.52319 (0.0)	-0.63918 (-0.0)	-0.37353 (-0.01035)
H(50)	N/A(N/A)	-0.07741 (0.0)	0.15198 (0.01199)
S(9)	-0.49955 (0.0)	-0.50386 (-0.0)	-0.49431 (0.02598)

## References

- [1] G. J. Kubas, *Inorg. Synth.*, **1979**, 19, 90
- [2] E. A. Pruss, B.S. Snyder, A.M. Stacy, *Angew. Chem. Int. Ed.* **1993**, 32, 256
- [3] <http://www.theochem.uni-stuttgart.de/pseudopotentials/>, D. Andrae, Diplomarbeit, 1989
- [4] D. Feller, *J. Comp. Chem.*, **1996**, 17, 1571
- [5] K.L. Schuchardt, B.T. Didier, T. Elsethagen, L. Sun, V. Gurumoorthi, J. Chase, J. Li, T.L. Windus, *J. Chem. Inf. Model.*, **2007**, 47, 1045
- [6] F. Weinhold and C. R. Landis, *Chem. Ed.: Res. & Pract.* (CERP; special "Structural Concepts" issue) **2001**, 2, 91
- [7] H. Inoue, J.X. Wang, K. Sasaki, R.R. Adzic, *J. Electroanal. Chem.*, **2003**, 554-555, 77